Journal Pre-proof

Direct in-vivo assessment of global and regional mechano-electric feedback in the intact human heart

Michele Orini, PhD, Peter Taggart, DSc FRCP, Anish Bhuva, MD, PhD, Neil Roberts, MD, Carmelo Di Salvo, MD FECTS, Martin Yates, MD, Sveeta Badiani, MRCP, Stefan Van Duijvenboden, PhD, Guy Lloyd, MD, Andrew Smith, FRCA, Pier D. Lambiase, PhD FRCP FHRS

PII: S1547-5271(21)00405-7

DOI: https://doi.org/10.1016/j.hrthm.2021.04.026

Reference: HRTHM 8773

To appear in: *Heart Rhythm*

Received Date: 31 December 2020

Revised Date: 23 April 2021

Accepted Date: 23 April 2021

Please cite this article as: Orini M, Taggart P, Bhuva A, Roberts N, Di Salvo C, Yates M, Badiani S, Van Duijvenboden S, Lloyd G, Smith A, Lambiase PD, Direct in-vivo assessment of global and regional mechano-electric feedback in the intact human heart, *Heart Rhythm* (2021), doi: https://doi.org/10.1016/j.hrthm.2021.04.026.

Simultaneous electro-mechanical mapping during acute LV loading

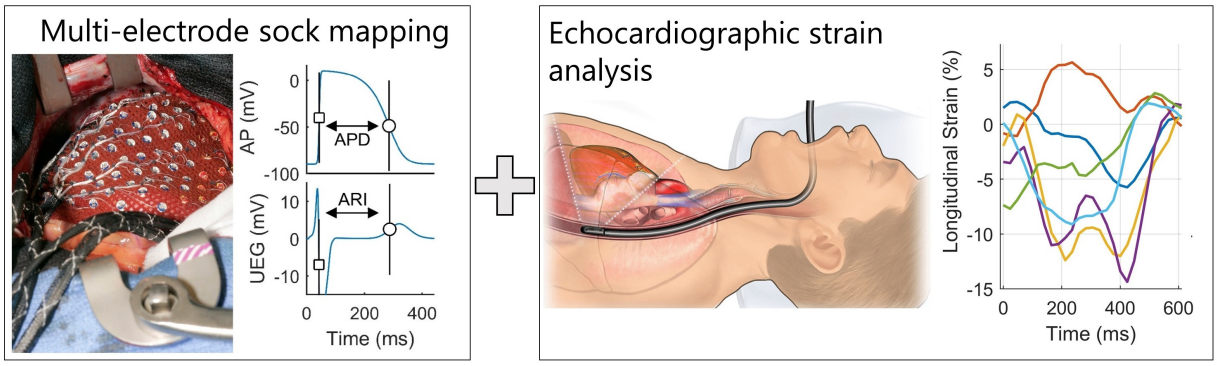

Inhomogeneity of contraction ⇨ Repolarization dispersion

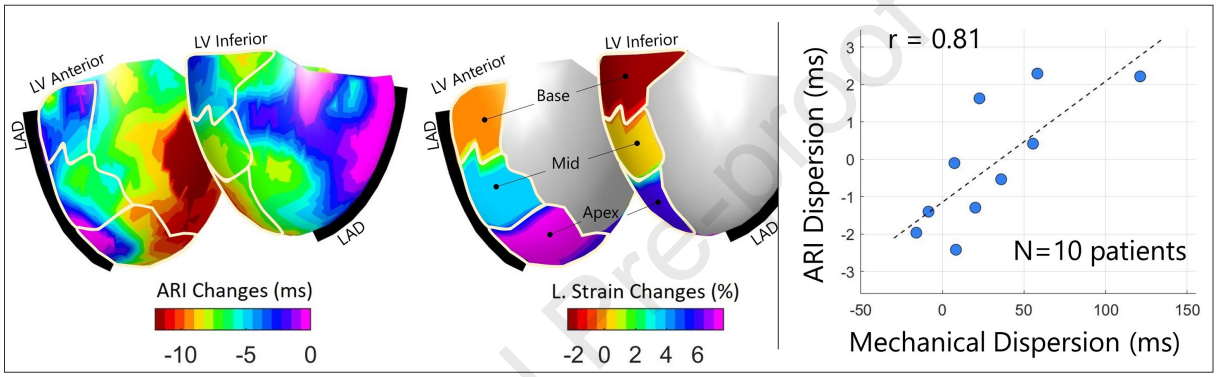

Direct in-vivo assessment of global and regional mechano-electric feedback in the intact human heart

Michele Orini[a,b], PhD; Peter Taggart[b,*] , DSc FRCP; Anish Bhuva[a,b], MD, PhD; Neil Roberts[a], MD; Carmelo Di Salvo[a], MD FECTS; Martin Yates[a], MD; Sveeta Badiani[a], MRCP; Stefan Van Duijvenboden[b], PhD; Guy Lloyd[a], MD; Andrew Smith[a], FRCA; Pier D. Lambiase[a,b] PhD FRCP FHRS

[*] Corresponding author

a: Barts Heart Centre at St Bartholomew's Hospital, London, UK

b: University College London, London, UK

Address for correspondence:

- Prof Peter Taggart, 5 University St, WC1E 6BT, London, UK; p.taggart@ucl.ac.uk;

Word count: 5070

Conflict of interest: Authors have no conflicts to disclose

Short title: Effect of mechanical deformation on human cardiac EP

Abstract

Background: Inhomogeneity of ventricular contraction is associated with sudden cardiac death, but the underlying mechanisms are unclear. Alterations in cardiac contraction impact electrophysiological parameters through mechano-electric feedback. This has been shown to promote arrhythmias in experimental studies, but its effect in the in-vivo human heart is unclear.

Objective: The aim of this study was to quantify the impact of regional myocardial deformation provoked by a sudden increase in ventricular loading (aortic occlusion) on human cardiac electrophysiology.

Methods: In ten patients undergoing open-heart cardiac surgery, left ventricular (LV) afterload was modified by transient aortic occlusion. Simultaneous assessment of whole-heart electrophysiology and LV deformation was performed using an epicardial sock (240 electrodes) and speckle-tracking transoesophageal echocardiography. Parameters were matched to six AHA LV model segments. The association between changes in regional myocardial segment length and in the activation-recovery interval (ARI, a conventional surrogate for action potential duration) was studied using mixed-effect models.

Results: Increased ventricular loading reduced longitudinal shortening (P=0.01) and shortened the ARI (P=0.02), but changes were heterogeneous between cardiac segments. Increased regional longitudinal shortening was associated with ARI shortening (effect size 0.20, 0.01 – 0.38, ms/% P=0.04) and increased local ARI dispersion (effect size -0.13, -0.23 – -0.03) ms/%, P=0.04). At the whole organ level, increased mechanical dispersion translated into increased dispersion of repolarization (correlation coefficient, r=0.81, P=0.01).

Conclusions: Mechano-electric feedback can establish a potentially pro-arrhythmic substrate in the human heart and should be considered to advance our understanding and prevention of cardiac arrhythmias.

Keywords: Mechano-electric feedback; Electromechanical coupling; Cardiac strain; Repolarization; Arrhythmia

Introduction

Mechano-electric feedback (MEF) is an established mechanism whereby myocardial deformation causes changes in cardiac electrophysiological parameters [1]. Animal, laboratory and theoretical investigations have demonstrated that abnormal patterns of cardiac deformation can modulate electrical excitation and recovery through MEF, which can be pro-arrhythmic [1–3]. Indeed, stretch activated ventricular arrhythmias are well-recognised clinical phenomena described in commotio cordis, mitral valve prolapse and infarct borderzones [4–8]. Furthermore, echocardiographic parameters of myocardial contractile function measured as strain (relative deformation of myocardial segments) and its spatial dispersion are established risk factors for ventricular arrhythmias in patients with impaired left ventricular (LV) function [9–11]. However, it remains unclear how mechanical perturbations commonly seen in these cardiac patients translate into a proarrhythmic electrophysiological substrate. The few studies that have tried to address this knowledge gap [12–15] have been limited to single site recordings which cannot capture mechanical desynchrony and spatial heterogeneity of electrophysiological parameters, which is a primary factor in the establishment of a pro-arrhythmic substrate. This is particularly important in view of the characteristically inhomogeneous nature of electrophysiological and mechanical properties of the human heart, which are known to be increased in pathological conditions. We hypothesised that global fluctuations in ventricular loading, common in cardiac conditions such as heart failure, are translated into regionally inhomogeneous changes in mechanical function which then induce regionally inhomogeneous changes in the electrophysiology by MEF thereby enhancing dispersion and creating a potentially pro-arrhythmic substrate.

In this study, we quantified the impact of regional myocardial deformation due to changes in left ventricular loading on electrical excitation and recovery in the *in-vivo* human heart. This was achieved through a unique experimental model that enabled simultaneous quantification

of electrophysiology (through high density, 240 electrodes, mapping) and cardiac mechanics (through speckle-tracking echocardiography) during manipulation of ventricular loading using the established method of transient aortic occlusion [12] in patients undergoing open heart surgery (Figure 1).

Methods

A detailed description of the methods is provided in the Supplementary Material.

Experimental setting

The study was approved by the local Ethics Committee (reference number 05/Q0502/45) and was conducted in accordance with the Declaration of Helsinki. All patients gave written informed consent. Cardiac mapping and transoesophageal echocardiography (TOE) were simultaneously performed in 10 patients (4 female, 63, 60-71 years old) undergoing cardiac surgery incorporating cardiopulmonary bypass [16,17] (7 coronary artery bypass grafting, 2 aortic valve replacement and 1 both). A multi-electrode heart sock enabling the recording of 240 unipolar electrograms was fit over the epicardium and aligned to the left anterior descending artery using landmarks and electrode labels to enable anatomical segmentation and co-registration with echocardiographic data. Ventricular pacing was established with pacing rate and pulses' duration and amplitude set to ensure consistent capture (20 bpm above sinus rhythm, 1 ms and twice the diastolic threshold, respectively, in most patients). A transient aortic clamp of 4-6 beats was performed to alter ventricular loading. If this induced ectopics, a second clamp was performed after 2 minutes. TOE recordings were taken before, during and after occlusion in a standard 2 chamber view using a Philips iE33 ultrasound machine enabling 2D speckle tracing for myocardial deformation analysis (Figure 1).

Data Analysis

Electrophysiological parameters

Activation (AT) and repolarization (RT) times were estimated from the unipolar electrograms using validated methods and activation recovery interval (ARI), an established measure of action potential duration (APD), was calculated as ARI = RT – AT [18,19] (Figure 1). Signal processing was performed with bespoke algorithms as in previous studies [19,20]. AT, ARI and RT from each electrode of the heart-sock were averaged during aortic occlusion and during 4 beats preceding and following it. Electrodes were matched to 6 segments of the AHA LV model for comparison with regional echocardiographic analysis (basal, mid and apical segments in the anterior and inferior portion of the LV). Mean and standard deviation of ARI across electrodes within each anatomical segment were computed to assess regional ARI and regional ARI dispersion, respectively. The range of regional ARI was computed as a measure of global electrophysiological dispersion. Assessment of regional AT and AT dispersion, as well as global AT dispersion, was conducted in the same way.

Echocardiographic parameters

TOE segments were analysed using commercial software integrating speckle tracking (TomTec Arena 1.4, TomTec Imaging Systems, Unterschleissheim, Germany). Image segmentation was performed semi-automatically by an expert cardiologist blinded to electrophysiological results, according to international consensus [21]. Deformation parameters were measured from a single beat showing stable waveforms. Myocardial segment length was measured in 6 AHA segments in the basal, mid and apical segments in the anterior and inferior portions of the LV. Change in myocardial segment length from end diastole to end systole as a percent of end diastolic length (strain) was measured. A negative value indicating segment shortening and a positive value indicating segment lengthening. For example, a segment of 1 cm that stretches to 1.5 cm or contracts to 0.5 cm would have +50% or -50%

strain, respectively. In sensitivity analysis, strain was measured as the fractional change in segment length from end diastole to its peak value within the cardiac cycle. Global mechanical dispersion was assessed as the standard deviation of time to peak change in myocardial segment length across the 6 anatomical segments [9].

Statistical analysis

Continuous variables are presented as median/interquartile range. The Wilcoxon sign-rank test was used to test paired comparisons (before vs during occlusion). Changes due to aortic occlusion were measured in terms of differences between parameters registered during and before occlusion. Correlation was assessed using the Spearman correlation coefficient. Mixed-effect regression models were used to study the association between electrophysiological changes and deformation parameters at the regional level. These models use data structured in a hierarchical way efficiently while reducing problems related to pseudo-replication. Electro-mechanical interactions across cardiac segments within the same subject were modelled as fixed effects, whereas inter-patient variability was considered as a random effect.

Results

In two patients, ectopic beats were induced during the first aortic clamp, but not during the second one. Increased ventricular loading increased LV cavity size and altered myocardial contractility and ventricular repolarization. An example from a representative patient is shown in Figure 2. Both ARI (panel A) and myocardial segment length (strain) (panel B) temporarily changed during increased ventricular loading (aortic occlusion). Our experimental model enabled simultaneous mapping and co-registration of ARI (panel C) and myocardial strain (panel D) changes over 6 LV segments.

Global effect of increased ventricular loading

Transient aortic occlusion induced significant changes in parameters describing global contractility and electrophysiology (Table 1). These included a significant reduction in LV ejection fraction (median variation of -15.6% compared to pre-occlusion, P=0.004) and in global longitudinal (P=0.01) and circumferential shortening (P=0.004) as well as in transverse thickening (P=0.014). These changes indicate a worsening of myocardial function with increased ventricular loading as compared to baseline conditions. ARI values changed by up to 15 ms during increased loading, the median ARI across the entire LV decreasing from 255 (228 – 268) ms before clamp to 252 (227 – 263) ms during clamp (P=0.02).

Correlation between regional cardiac deformation and electrophysiology

Regional changes in myocardial deformation and repolarization were heterogeneous. The ARI decrease was not uniformly distributed across the LV. While the median ARI decrease across patients was equal to 4 (3 – 5) ms, some cardiac sites showed substantial reductions in ARI, with the maximal ARI decreases of 15 (13 – 20) ms. At the same time, 18.3% of all cardiac segments showed an increase in ARI. Similarly, although longitudinal segment shortening was decreased during occlusion in most segments, 36.7% of all segments showed an increase in longitudinal segment shortening. At the regional level, changes in longitudinal segment shortening significantly correlated to regional ARI and ARI dispersion (i.e. spatial heterogeneity of repolarization). Mixed-effect models identified a significant positive association between changes in ARI and changes in longitudinal strain (effect size 0.20 (0.01/0.38) ms/%, P=0.04). This indicates regional ARI reduction in segments with increased longitudinal shortening and regional ARI increase in segments with reduced longitudinal shortening (Figure 3A). Changes in longitudinal shortening were also significantly associated with changes in regional ARI dispersion (effect size -0.13 (-0.23/-0.03) ms/%, P=0.01). This

indicates that spatial heterogeneity of ARI increased in segments with greater longitudinal shortening (Figure 3B).

Regional changes in longitudinal segment length at baseline, i.e. before transient aortic clamping, was associated with regional ARI (P=0.067) and regional ARI dispersion (P=0.024) (Supplementary Table 1). No significant associations were identified between regional myocardial deformation parameters and regional activation time (AT), whereas changes in total repolarization (i.e. RT=AT+ARI) showed associations with myocardial deformation parameters akin to those described for ARI (Supplementary Table 1).

At the patient level, changes in global dispersion of ARI (i.e. ARI heterogeneity between segments) strongly correlated to mechanical dispersion (r = 0.81, P = 0.01, Figure 4). This indicates that increased mechanical desynchrony translated into increased dispersion of repolarization. A moderate but nonsignificant correlation was also found between global dispersion of ARI and the standard deviation of longitudinal strain between segments (r = 0.50, P = 0.14).

Sensitivity analysis conducted using peak strain values showed similar results (Supplementary Table 2). Regional longitudinal strain remained significantly implicated in the changes observed in regional ARI and regional ARI dispersion and the effect sizes were similar.

Activation-repolarization interactions

Experimental models in animals have shown that the normal inverse relationship between activation time and repolarisation time is modulated by alterations in ventricular loading [22]. In the current study, across electrodes covering the LV, maximum ARI shortening was significantly greater for sites activating late (i.e. after median activation time) than for sites activating early (i.e. before median activation time) at 14.2 (11.5 – 20.3) ms versus 12.4 (9.3

– 13.7) ms, P=0.01, respectively. The median value of ARI shortening for late activated LV sites was numerically greater than for early activated ones, at 4.2 (2.5 – 6.04) ms vs 3.3 (2.7 – 4.3) ms, but the difference was not statistically significant, P=0.19.

Discussion

This study provides a quantitative and simultaneous assessment of the effect of myocardial deformation on ventricular electrophysiology during a sudden change in ventricular loading. The transient aortic occlusion utilised in this model to alter ventricular loading significantly modified contractility (longitudinal, transverse and circumferential myocardial strain) and the electrophysiology. The main findings of the study are that (1) Global changes in ventricular loading produce regional changes in mechanical function and electrophysiology which were inhomogeneous. (2) Changes in regional longitudinal shortening were directly related to changes of both regional repolarization and regional repolarization dispersion and (3) Global mechanical dispersion, a measurement of desynchrony in contraction, increased global dispersion of repolarization. These results are consistent with the hypothesis that increase in ventricular loading produces inhomogeneous changes in both mechanical function and the electrophysiology between different regions as well locally within regions through the intermediary of MEF. This is especially important in the presence of underlying heart disease, such as ischaemic heart disease and cardiomyopathy, which are characteristically associated with the development of scar and fibrosis, both of which are patchy and promote contraction inhomogeneity. These results have important implications in the understanding of fundamental mechanisms underlying potentially life-threating ventricular arrhythmias in the human heart, because they implicate impaired myocardial contraction and desynchrony in the modulation of regional and global spatial dispersion of repolarization, which are well-established pro-arrhythmic factors [23–25]. This could at least partially explain the association

198 between mechanical dispersion and ventricular arrhythmia or sudden cardiac death,
199 established from clinical studies [9–11].

200 The analysis of regional mechano-electric interactions shows that changes in the mechanical
201 properties of a given cardiac segment not only directly impact on the electrophysiology of the
202 same segment (Figure 3), but may also affect the electrophysiology of spatially distinct but
203 coupled segments as suggested by laboratory preparations [26]. This could explain why there
204 was no significant association between time-to-peak change in myocardial segment length
205 and repolarization at the regional level (i.e. on the same segment), but there was a significant
206 correlation between global mechanical dispersion and global dispersion of repolarization
207 (Figure 4).

208 A previous study using a similar model of increased afterload in patients found a reduction in
209 the action potential duration, which correlated with peak systolic pressure [12]. However,
210 regional MEF interactions were not assessed due to lack of echocardiographic data and
211 simultaneous multi-sites cardiac mapping. The overall mean reduction of ARI during
212 increased loading in the present study using multisite recordings is consistent with the mean
213 reduction in APD in the previous study using single site recordings. However, it was not
214 appreciated in the earlier work that a significant number of areas in the heart may show an
215 opposite response during loading, i.e. an increase in ARI during loading as observed in 18.3%
216 of sites in the present study. Our results indicate that global parameters alone may not be
217 sufficient to characterise mechano-electric coupling and that physiological behaviour may be
218 masked by global averaging and suggest that while single site recordings provide valuable
219 information they need to be complemented with multisite information.

MEF mechanisms

Changes in the mechanical environment of the myocardial cell influence the APD by MEF pathways involving stretch activated channels, calcium cycling and chemical signalling [27–31]. The effect of each of these mechanisms on ventricular repolarization is strongly dependent on the nature and timing of the mechanical perturbation. Although the temporal resolution of echocardiography did not allow to accurately assess the effect of the temporal pattern of myocardial deformation on repolarization changes, we found greater peak ARI reduction in late-activated LV segments as compared to early-activated segments.

Although experimental work on cells, tissues, and *in silico* has identified a range of cellular mechanisms and electrophysiological responses to specific alterations in ventricular loading, extrapolation to the in-vivo human heart is challenging in view of the three-dimensional complexity of the stress/strain relationships during the cardiac cycle and species differences in cardiomyocyte electrophysiology and species-dependent mechanisms underlying arrhythmias [32]. In this study, we have incorporated a model of increased afterload, as increased afterload is commonly encountered clinically in pathological conditions both on a global and regional scale. We observed a predominant shortening of ventricular APD with some regions showing lengthening occurring immediately following the abrupt onset of increased afterload. Possible mechanisms would include stretch activated non-specific cation channels (SACns) [30]. SACns have a reversal potential at approximately -30 mV such that SACs activated at membrane potentials positive to the reversal potential, i.e. during the plateau phase, shorten APD and SACs activated at more negative potential, i.e. during the later repolarisation phase, prolong APD [28,30]. Another possible mechanism would be the effect of increased afterload on calcium cycling. Myocardial shortening decreases the affinity of Ca^{2+} for troponin C [3]. Free sarcoplasmic calcium during the late phase of the action potential is higher in shortened than non-shortened myocardial segments which would be

expected to prolong the action potential by Na-Ca exchange. Therefore, the more isometric contraction associated with the aortic cross clamping model would be expected to promote the opposite effect, i.e. APD shortening [3,27,28,31]. Recent work has shown that altered mechanical loading may induce rapid local Ca^{2+} release that is not reflected in global Ca^{2+} but confined to localised regions such as the narrow dyadic space between ryanodine receptors and the L type Ca^{2+} channels [3,33–35]. This microdomain microsensitivity includes reactive oxygen species and NO pathway signalling. While NO signalling tends to operate on a longer time scale it is possible that the rapid effect of X-ROS signalling in enhancing the efficiency of calcium induced calcium release may play a role and contribute to arrhythmogenesis by inducing early and delayed afterdepolarisations through sodium/calcium exchange.

Clinical implications

Stretch activated ventricular arrhythmias are a well-recognised phenomenon in clinical practice including ventricular fibrillation triggered by commotio cordis. Indeed, recently, the role of stretch activated premature ventricular contractions has become recognised as a mechanism of triggering VF in mitral valve prolapse [8]. Dispersion of repolarisation is linked to heterogeneities in mechanical dysfunction promoting mechano-electric differences in ion channelopathies such as Long QT syndrome. However, the fact that myocardial infarction is much more common implicates the pro-arrhythmic effects of stretch in the infarct border-zone or dyssynchronous ventricle of left bundle branch block as a pro-arrhythmic mechanism more widely in the population.

Mechanisms of arrhythmogenesis in the infarct border-zone operate on a number of levels including activation of stretch activated channels that change APD, slow conduction velocity, or increase dispersion of repolarization on the physiological level, to changes in expression of mechanically modulated ion channels and alterations in connexin phosphorylation at the molecular level through to structural remodelling of tissue architecture, composition and

innervation [4–7]. These processes conspire to further promote arrhythmogenicity in the infarct border-zone in response to stretch. Indeed, variability in the site and degree of stretch in this region can create dispersion of repolarization to enable the initiation of ventricular tachycardia. This region is the target of catheter ablation which usually focuses on the electrophysiological markers of structural disease and conduction slowing as opposed to regions of increased strain influencing repolarization.

Mechanical deformation parameters are also becoming recognised predictors of arrhythmic events in structural heart disease [9–11]. These could potentially be improved by integration with markers of repolarization dispersion in sites of abnormal strain/increased mechanical dispersion.

Limitations

The number of patients included in the study was limited by the inherent difficulty of conducting experimental studies including electrophysiological and speckle-tracking recordings in the cardiac theatre. However, the statistical methods utilised make an efficient use of the data and detected significant associations. Co-registration of regional strain and electrophysiological data was performed using anatomical landmarks and labels on the heart-sock, but remaining imprecision may have affected the results, possibly reducing the significance of some associations. Measurement of electrophysiological and strain parameters may be challenging in some cases. However, to ensure accuracy and robustness, analyses were performed independently utilising validated software, automatic exclusion of outliers was performed using pre-determined criteria and sensitivity analysis has been conducted to check for consistency. We cannot exclude the possibility that placement of the sock around the heart may influence the electrophysiology. However, the sock fits gently around the heart and if any mechanically induced repolarisation changes were induced by its placement, we would expect them to be trivial.

Conclusion

This study developed a unique in-vivo in-human experimental model of acutely increased ventricular loading by combining multisite electrophysiological mapping with simultaneous transoesophageal ultrasound and an established aortic cross clamping protocol in patients undergoing cardiac surgery. The results show that global ventricular loading conditions induce regional differences in myocardial shortening. These changes in myocardial shortening are associated with changes in the electrophysiology most probably by MEF whereby increased mechanical dispersion results in greater dispersion of repolarization. This suggests that mechano-electric feedback can contribute to the establishment of pro-arrhythmic substrates in patients and provides a mechanistic explanation for the association between myocardial strain parameters and sudden cardiac death reported in clinical studies.

Acknowledgements

This work was supported by the Medical Research Council (UK) [G0901819], the Marie Curie Intra-European Fellowship [FP7-PEOPLE-2013-IEF 622889 to M.O.], University College London Hospitals (UCLH) Biomedicine NIHR and Barts BRC.

References

1. Kohl P, Ravens U: Cardiac mechano-electric feedback: Past, present, and prospect. Prog Biophys Mol Biol 2003; 82:3–9.

2. Kohl P, Hunter P, Noble D: Stretch-induced changes in heart rate and rhythm: clinical observations, experiments and mathematical models. Prog Biophys Mol Biol 1999; 71:91–138.

3. Alexander Quinn T, Kohl P: Cardiac mechano-electric coupling: Acute effects of

mechanical stimulation on heart rate and rhythm. Physiol Rev American Physiological Society, 2021; 101:37–92.

4. Quintanilla JG, Moreno J, Archondo T, et al.: Increased intraventricular pressures are as harmful as the electrophysiological substrate of heart failure in favoring sustained reentry in the swine heart. Heart Rhythm Elsevier, 2015; 12:2172–2183.

5. Franz MR, Burkhoff D, Yue DT, Sagawa K: Mechanically induced action potential changes and arrhythmia in isolated and in situ canine hearts. Cardiovasc Res 1989; 23:213–223.

6. Ashikaga H, Mickelsen SR, Ennis DB, et al.: Electromechanical analysis of infact border zone in chronic myocardial infarction. Am J Physiol Circ Physiol 2005; 289:H1099-105.

7. John B, Stiles MK, Kuklik P, et al.: Reverse Remodeling of the Atria After Treatment of Chronic Stretch in Humans. Implications for the Atrial Fibrillation Substrate. J Am Coll Cardiol Elsevier, 2010; 55:1217–1226.

8. Basso C, Iliceto S, Thiene G, Perazzolo Marra M: Mitral Valve Prolapse, Ventricular Arrhythmias, and Sudden Death. Circulation 2019; 140:952–964.

9. Haugaa KH, Smedsrud MK, Steen T, et al.: Mechanical Dispersion Assessed by Myocardial Strain in Patients After Myocardial Infarction for Risk Prediction of Ventricular Arrhythmia. JACC Cardiovasc Imaging Elsevier Inc., 2010; 3:247–256.

10. Haugaa KH, Grenne BL, Eek CH, et al.: Strain echocardiography improves risk prediction of ventricular arrhythmias after myocardial infarction. JACC Cardiovasc Imaging JACC Cardiovasc Imaging, 2013; 6:841–850.

11. Perry R, Patil S, Marx C, et al.: Advanced Echocardiographic Imaging for Prediction

of SCD in Moderate and Severe LV Systolic Function. JACC Cardiovasc Imaging Elsevier Inc., 2020; 13:604–612.

12. Taggart P, Sutton P, Lab M, Runnalls M, O'Brien W, Treasure T: Effect of abrupt changes in ventricular loading on repolarization induced by transient aortic occlusion in humans. Am J Physiol Circ Physiol 1992; 263:H816–H823.

13. Taggart P, Sutton P, John R, Lab M, Swanton H: Monophasic action potential recordings during acute changes in ventricular loading induced by the Valsalva manoeuvre. Br Heart J 1992; 67:221–229.

14. Chen Z, Hanson B, Sohal M, et al.: Coupling of ventricular action potential duration and local strain patterns during reverse remodeling in responders and nonresponders to cardiac resynchronization therapy. Heart Rhythm 2016; 13:1898–1904.

15. Orini M, Nanda A, Yates M, et al.: Mechano-electrical feedback in the clinical setting: Current perspectives. Prog Biophys Mol Biol 2017; 130:365–375.

16. Orini M, Taggart P, Srinivasan N, Hayward M, Lambiase PDPD: Interactions between activation and repolarization restitution properties in the intact human heart: In-vivo whole-heart data and mathematical description. PLoS One 2016; 11:e0161765.

17. Taggart P, Orini M, Hanson B, et al.: Developing a novel comprehensive framework for the investigation of cellular and whole heart electrophysiology in the in situ human heart: Historical perspectives, current progress and future prospects. Prog Biophys Mol Biol 2014; 115:252–260.

18. Orini M, Srinivasan N, Graham AJ, Taggart P, Lambiase PD: Further Evidence on How to Measure Local Repolarization Time Using Intracardiac Unipolar Electrograms in the Intact Human Heart. Circ Arrhythmia Electrophysiol 2019; 12.

19. Orini M, Taggart P, Lambiase PD: In vivo human sock-mapping validation of a simple model that explains unipolar electrogram morphology in relation to conduction-repolarization dynamics. J Cardiovasc Electrophysiol 2018; 29:990–997.

20. van Duijvenboden S, Hanson B, Child N, et al.: Pulse Arrival Time and Pulse Interval as Accurate Markers to Detect Mechanical Alternans. Ann Biomed Eng Springer New York LLC, 2019; 47:1291–1299.

21. Voigt JU, Pedrizzetti G, Lysyansky P, et al.: Definitions for a common standard for 2D speckle tracking echocardiography: Consensus document of the EACVI/ASE/industry task force to standardize deformation imaging. J Am Soc Echocardiogr Mosby Inc., 2015; 28:183–193.

22. Opthof T, Meijborg VMF, Belterman CNW, Coronel R: Synchronization of repolarization by mechano-electrical coupling in the porcine heart. Cardiovasc Res 2015; 108:181–187.

23. Kuo CS, Munakata K, Reddy CP, Surawicz B: Characteristics and possible mechanism of ventricular arrhythmia dependent on the dispersion of action potential durations. Circulation 1983; 67:1356–1367.

24. Coronel R, Wilms-Schopman FJG, Opthof T, Janse MJ: Dispersion of repolarization and arrhythmogenesis. Heart Rhythm Elsevier, 2009; 6:537–543.

25. Laurita KR, Girouard SD, Akar FG, Rosenbaum DS: Modulated dispersion explains changes in arrhythmia vulnerability during premature stimulation of the heart. Circulation Lippincott Williams and Wilkins, 1998; 98:2774–2780.

26. Solovyova O, Katsnelson LB, Kohl P, Panfilov A V., Tsaturyan AK, Tsyvian PB: Mechano-electric heterogeneity of the myocardium as a paradigm of its function. Prog

Biophys Mol Biol 2016; 120:249–254.

27. Lab MJ: Contraction-excitation feedback in myocardium. Physiological basis and clinicl relevance. Circ Res 1982; 50:757–766.

28. Kohl P, Day K, Noble D: Cellular mechanisms of cardiac mechano-electric feedback in a mathematical model. Can J Cardiol 1998; 14:111–119.

29. Taggart P, Sutton PMI: Cardiac mechano-electric feedback in man: Clinical relevance. Prog Biophys Mol Biol Elsevier Ltd, 1999; 71:139–154.

30. Peyronnet R, Nerbonne JM, Kohl P: Cardiac Mechano-Gated Ion Channels and Arrhythmias. Circ Res Lippincott Williams and Wilkins, 2016; 118:311–329.

31. Johnson DM, Antoons G: Arrhythmogenic mechanisms in heart failure: Linking β-adrenergic stimulation, stretch, and calcium. Front. Physiol. Frontiers Media S.A., 2018, p. 1453.

32. Edwards AG, Louch WE: Species-dependent mechanisms of cardiac arrhythmia: A cellular focus. Clin Med Insights Cardiol SAGE Publications, 2017; 11:1179546816686061.

33. Iribe G, Ward CW, Camelliti P, et al.: Axial stretch of rat single ventricular cardiomyocytes causes an acute and transient increase in Ca2+ spark rate. Circ Res Circ Res, 2009; 104:787–795.

34. Belmonte S, Morad M: Shear fluid-induced Ca2+ release and the role of mitochondria in rat cardiac myocytes. Ann N Y Acad Sci Blackwell Publishing Inc., 2008, pp. 58–63.

35. Prosser BL, Ward CW, Lederer WJ: X-ROS signaling: Rapid mechano-chemo transduction in heart. Science (80-) Science, 2011; 333:1440–1445.

410

411

Figures

Figure 1

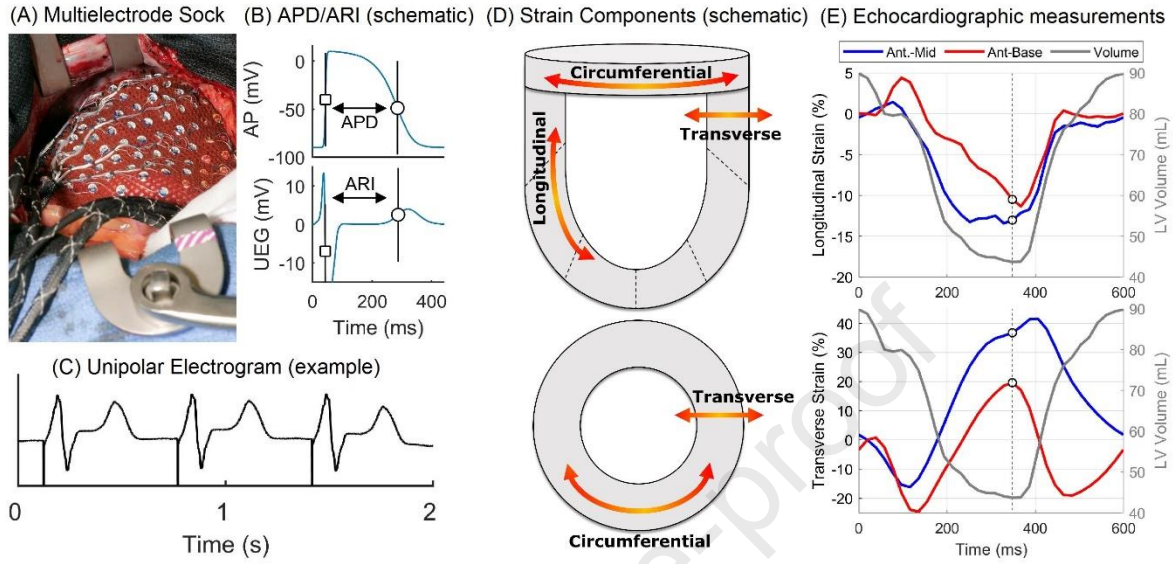

Figure 1: A: Epicardial sock placed around a patient's heart during surgery (adapted from [17]). B: Activation recovery interval (ARI), a surrogate for action potential duration (APD), is measured from unipolar electrograms (UEG) as the difference between activation (square) and repolarization (circle) times. C: Representative examples of unfiltered unipolar electrograms. D: Schematic showing longitudinal, transverse and circumferential components of myocardial deformation. E: Fractional change in longitudinal and transverse segment length (strain) are illustrated for 2 cardiac segments (anterior base, red, and anterior-mid myocardium, blue) along with intraventricular volume (solid grey line). Measurements were taken at end systolic volume (dotted vertical line). Note that longitudinal strain values are negative, indicating a relative shortening.

426 Figure 2

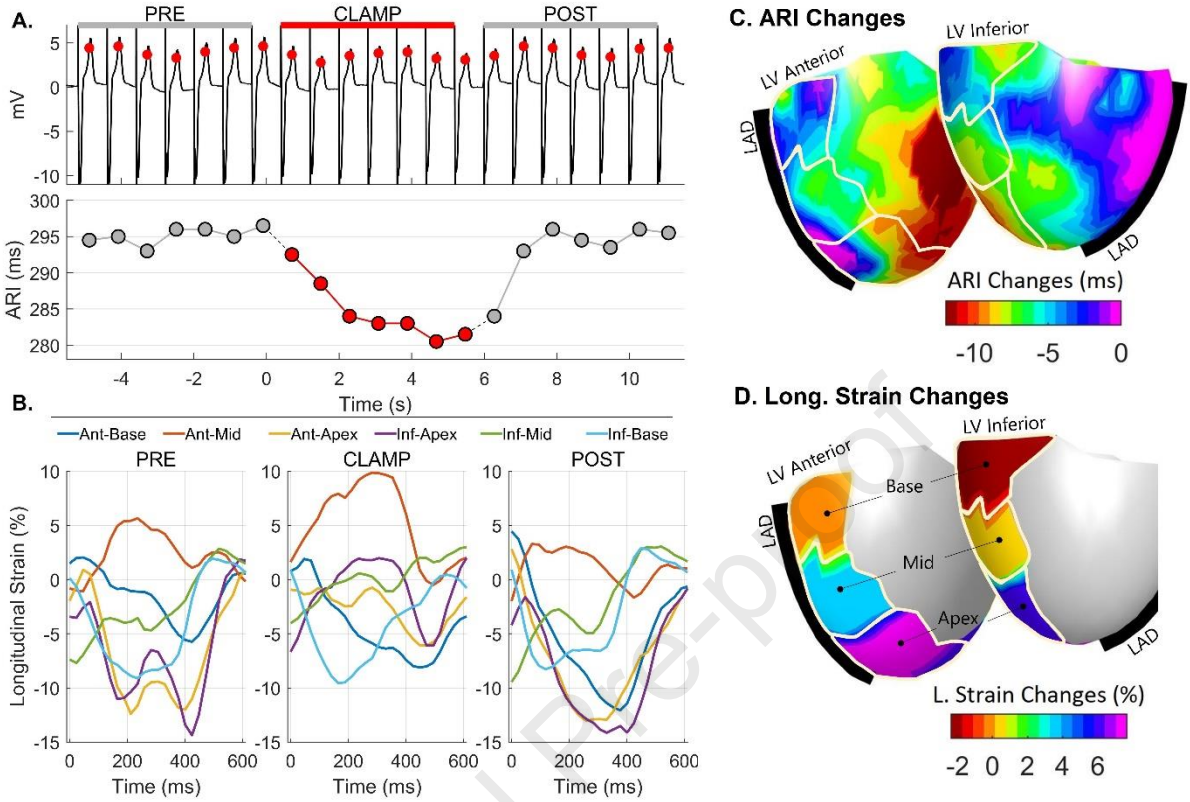

427

428 **Figure 2**: Example of the effect of transient aortic occlusion on electrophysiological and
429 myocardial deformation parameters in a representative patient. A: Unipolar electrograms with
430 repolarization time markers (red circles, upper panel) and activation-recovery interval (ARI,
431 below) before, during (red) and after occlusion. B: Waveforms representing longitudinal
432 strain in 6 left ventricular segments of the standardized AHA left ventricular model during a
433 single cardiac cycle before, during and after occlusion. C: Changes in ARI during aortic
434 clamp mapped over the heart-sock geometry. D: Changes in longitudinal strain during aortic
435 clamp mapped over the heart-sock geometry. A stylized left anterior descending artery
436 (LAD) and LV AHA segments are reported for orientation.

437 Figure 3

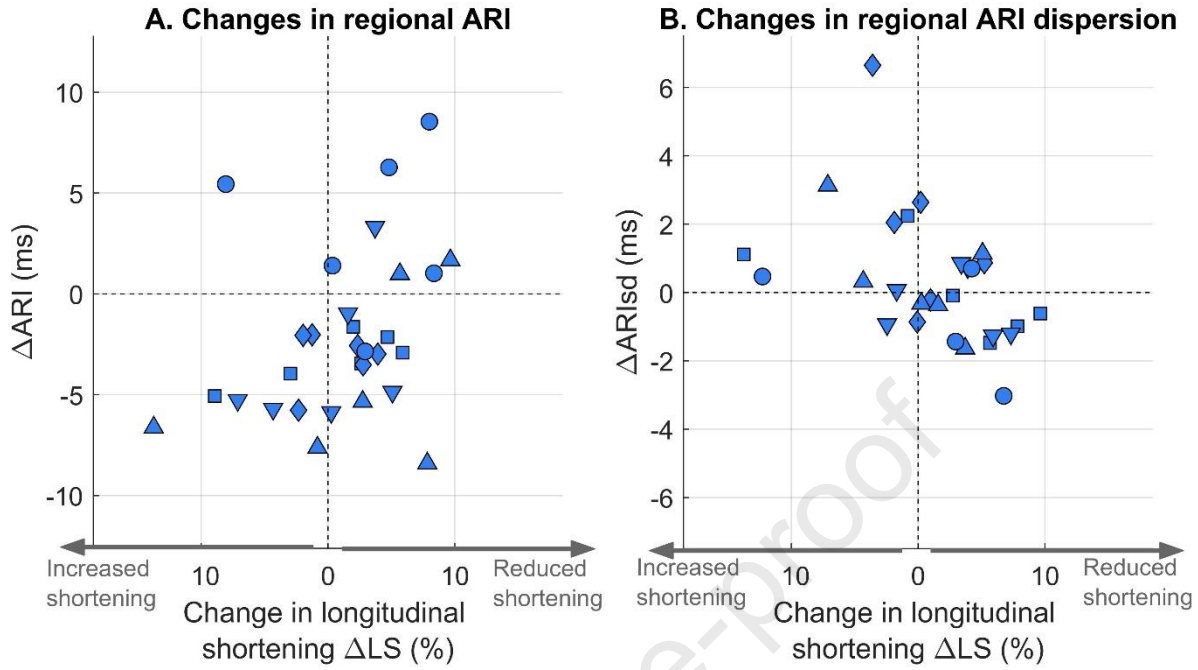

438

439 **Figure 3:** Correlation between myocardial deformation and repolarization secondary to
440 increase in ventricular loading for n=5 patients. Each symbol represents a cardiac segment
441 and each marker type represents a patient (6 cardiac segments per patient). Changes in
442 regional longitudinal (ΔLS) correlated with changes in regional ARI (ΔARI) and inversely
443 correlated with changes in regional ARI dispersion (ΔARIsd).

444

445

446 Figure 4

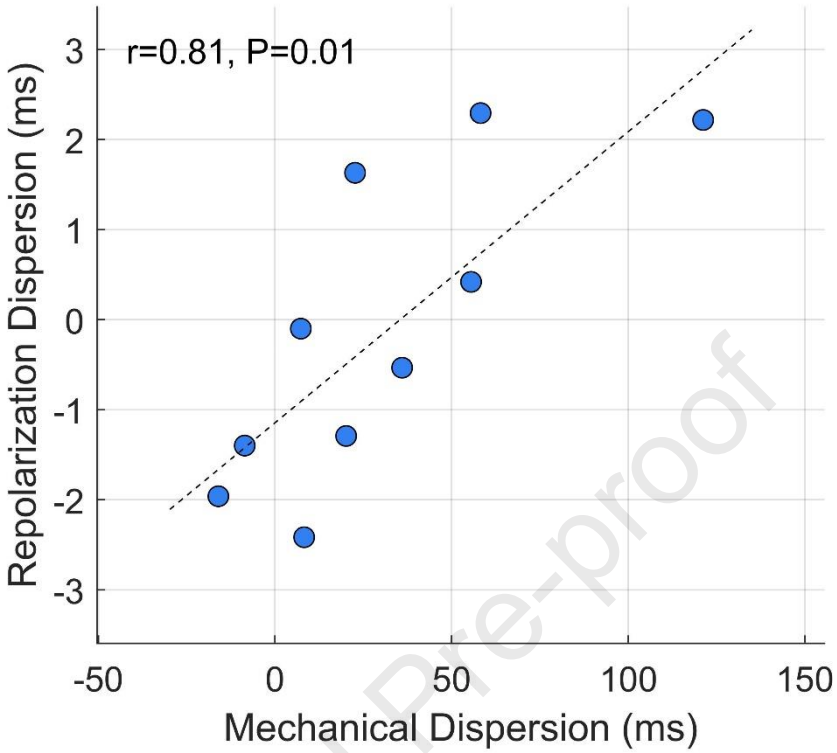

447

448 **Figure 4:** Translation of global mechanical dispersion into global electrophysiological
449 dispersion. During increase in ventricular loading, changes in mechanical dispersion,
450 measured as the standard deviation of time to peak longitudinal shortening (strain), correlated
451 with global ARI dispersion, measured as the standard deviation of regional ARI. Each
452 symbol represents a patient (n=10). The correlation coefficient, r, is reported for each
453 scatterplot.

454

455

Tables 1

		Pre	Occlusion	Post
LV ARI (mean)	ms	255 (228-268)	**252 (227-263)** *	254 (230-269)
LV ARI (SD)	ms	16.0 (13.5-19.5)	16.8 (13.7-18.4)	17.0 (13.7-19.9)
LV AT (mean)	ms	49.6 (43.1-52.5)	49.7 (42.8-52.5)	49.4 (43.1-53.5)
LV AT (SD)	ms	22.2 (17.2-23.5)	22.3 (17.4-23.4)	22.2 (17.1-23.5)
LV RT (mean)	ms	306 (288-315)	**302 (282-311)** **	305 (288-316)
LV RT (SD)	ms	21.8 (18.7-29.5)	23.0 (18.4-29.5)	22.7 (18.7-30.5)
EDV	ml	99.6 (89.5-135.1)	110.0 (72.1-143.8)	109.5 (94.0-131.1)
ESV	ml	48.8 (43.8-83.3)	57.5 (46.2-92.5)	56.4 (35.2-88.2)
LVEF	%	44.9 (41.5-51.6)	**37.9 (33.5-46.8)** **	47.8 (42.8-59.7)
GLS	%	-9.69 (-11.30--6.55)	**-6.77 (-9.76--4.77)** **	-10.74 (-18.24--5.92)
GCS	%	-19.9 (-21.5--16.6)	**-14.0 (-18.1--13.1)** **	-17.5 (-25.7--13.3)
GRS	%	23.7 (14.4-27.3)	**18.2 (9.8-19.9)** *	18.4 (9.7-30.6)

Table 1: Global parameters of myocardial deformation and electrophysiology before (Pre) during (Occlusion) and after (Post) transient aortic occlusion. Values are reported as median (1^{st} – 3^{rd} quartile) across patients (n=10). Values statistically different from pre-occlusion are reported in bold (*:P<0.05; **:P<0.01). Electrophysiological parameters are measured as mean and standard deviation (SD) across all electrodes covering the left ventricle. ARI: Activation-recovery interval; AT and RT: Activation and repolarization time; EDV and ESV: End diastolic and systolic volumes; GLS, GCR and GRS: Global longitudinal, circumferential and radial strain, respectively. LVEF: Left ventricular ejection fraction.